Hydrogen Peroxide Removes TRPM4 Current Desensitization Conferring Increased Vulnerability to Necrotic Cell Death*[S]

Felipe Simon[1,2]**, Elías Leiva-Salcedo**[1]**, Ricardo Armisén**[1]**, Ana Riveros, Oscar Cerda, Diego Varela, Ana Luisa Eguiguren, Pablo Olivero**[3]**, and Andrés Stutzin**[4]

From the Centro de Estudios Moleculares de la Célula and Instituto de Ciencias Biomédicas, Facultad de Medicina, Universidad de Chile, Av. Independencia 1027, Independencia 838-0543, Santiago, Chile

Necrosis is associated with an increase in plasma membrane permeability, cell swelling, and loss of membrane integrity with subsequent release of cytoplasmic constituents. Severe redox imbalance by overproduction of reactive oxygen species is one of the main causes of necrosis. Here we demonstrate that H_2O_2 induces a sustained activity of TRPM4, a Ca^{2+}-activated, Ca^{2+}-impermeant nonselective cation channel resulting in an increased vulnerability to cell death. In HEK 293 cells overexpressing TRPM4, H_2O_2 was found to eliminate in a dose-dependent manner TRPM4 desensitization. Site-directed mutagenesis experiments revealed that the Cys[1093] residue is crucial for the H_2O_2-mediated loss of desensitization. In HeLa cells, which endogenously express TRPM4, H_2O_2 elicited necrosis as well as apoptosis. H_2O_2-mediated necrosis but not apoptosis was abolished by replacement of external Na^+ ions with sucrose or the non-permeant cation N-methyl-D-glucamine and by knocking down TRPM4 with a shRNA directed against TRPM4. Conversely, transient overexpression of TRPM4 in HeLa cells in which TRPM4 was previously silenced re-established vulnerability to H_2O_2-induced necrotic cell death. In addition, HeLa cells exposed to H_2O_2 displayed an irreversible loss of membrane potential, which was prevented by TRPM4 knockdown.

The transient receptor potential (TRP)[5] ion channel superfamily comprises a broad variety of cation-selective channels key to many physiological processes, including sensation, cell proliferation, and cell death (1, 2). TRPM4 is a Ca^{2+}-activated and voltage-dependent monovalent cation selective channel corresponding to the melastatin subfamily of TRP channels (3).

A distinct feature of TRPM4, as well as TRPM5 channels is that upon activation by intracellular Ca^{2+}, currents exhibit a fast decay due to a decrease in the sensitivity to Ca^{2+} (3–6). In addition, these channels have been shown to depend on phosphatidylinositol 4,5-bisphosphate ($PI(4,5)P_2$) (7, 8), suggesting that the current decay or desensitization of TRPM4 can be explained partially by a loss of $PI(4,5)P_2$ from the channels.

TRPM4 features similar biophysical and pharmacological properties to Ca^{2+}-activated, Ca^{2+}-impermeable nonselective cation channels (CAN) described in many excitable and nonexcitable cells (9, 10). CAN channels are widely expressed among different tissues exhibiting several common characteristics, such as a low open probability when studied *in situ*, a conductance of 15–30 pS under symmetrical Na^+ conditions, and a weak voltage-dependent gating. In addition, these channels are activated by intracellular Ca^{2+} and blocked by ATP, suggesting that their activation may be coupled to the metabolic status of the cell. Furthermore, some CAN channels have been found to be activated by reactive oxygen species (ROS) in a number of cell types (11–17). Because of their ion selectivity, an unregulated activation of CAN channels may have detrimental consequences for cell homeostasis, expressed by a collapse of the Na^+ and K^+ transmembrane gradients, a reduction of the membrane potential, and an increased turnover rate of the Na^+/K^+-ATPase pump and thus, increased ATP consumption. Several of these conditions observed under oxidative stress may lead to necrotic cell death. Thus, distinctive and necessary events are membrane depolarization and cell swelling, a phenomenon known as necrotic volume increase (18, 19). Indeed, pharmacological inhibition of these channels prevents cytosolic Na^+ and Ca^{2+} overload, cell volume increase, and death of liver and neuronal cells exposed to oxidative damage (15, 20). More recently, Gerzanich *et al.* (21) demonstrated that *in vitro* expression of TRPM4, a molecular candidate for CAN channels as previously suggested (10, 22), predisposes to cell death upon ATP depletion.

In this work we addressed the question whether TRPM4 is modulated by ROS. Here we show that the Cys[1093] residue participates in mediating the effect of H_2O_2 on TRPM4 current desensitization. As a result, the transmembrane potential collapses eventually leading to severe metabolic derangement and subsequent cell death.

EXPERIMENTAL PROCEDURES

Cell Culture and Cells—T-REx-293 cells, a HEK 293-derived cell line, were obtained from Invitrogen and cultured in

DMEM/F-12 (Invitrogen) supplemented with 5% fetal bovine serum (FBS) and 2 mM glutamine. HeLa cells were obtained from ATCC (Manassas, VA) and cultured in DMEM, low glucose supplemented with 5% FBS and 2 mM glutamine. Both cell lines were maintained in a 95% air, 5% CO_2 atmosphere at 37 °C, passaged twice a week and used from passages 5–10.

Tetracycline-inducible T-REx-293 hTRPM4 Cells—The full-length human TRPM4b cDNA containing a FLAG epitope tag in the N terminus was cloned into a modified version of the pcDNA4/TO vector (Invitrogen) and transfected into T-REx-293 cells that stably express plasmid pcDNA6/TR for Tet-repressor expression (Invitrogen). Cells were placed under zeocin selection and zeocin-resistant clones were screened for tetracycline-inducible expression of the FLAG-tagged TRPM4 protein. The medium was supplemented with blasticidin (5 μg/ml, Invitrogen) and zeocin (0.4 mg/ml, Invitrogen). For most experiments, cells were resuspended in medium containing 1 μg/ml of tetracycline (Invitrogen) 18–24 h before experiments. For electrophysiological experiments cells were plated on coverslips and 1 μg/ml of tetracycline was added for 16–24 h before performing experiments.

shRNA-TRPM4 HeLa Cell Clones—A short-hairpin RNA for TRPM4 was constructed according to Ref. 23. Briefly, 64-mer primers were designed to include a 19-mer TRPM4 sequence (24), its complement, a spacer region, 5′ BglII site and 3′ HindIII sites. A scrambled duplex was used as a control. The annealed double-stranded DNA was cloned into the pSUPER.retro.neo vector (Oligoengine, Seattle, WA) and HeLa cells were transfected with Lipofectamine 2000 (Invitrogen) and placed under G418 (Sigma) selection. G418-resistant clones were screened for TRPM4 mRNA reduction and clones were kept in a medium supplemented with G418 (0.5 mg/ml; Invitrogen).

Quantitative PCR—RT and qPCR were performed to measure TRPM2, TRPM4, TRPM7, and the housekeeping gene GADPH mRNA levels in HeLa cells using the primers described in Ref. 25. Total RNA was extracted with TRIzol according to the manufacturer's protocol (Invitrogen). DNase I-treated RNA was used for reverse transcription using the SuperScript II kit (Invitrogen). Equal amounts of RNA were used as templates in each reaction. qPCR was performed using SYBR Green PCR Master Mix (AB Applied Biosystems, Foster City, CA). Data are presented as relative mRNA levels of the gene of interest normalized to relative levels of GADPH mRNA. These values were calculated from a standard curve generated with HeLa wild type cDNA.

Site-directed Mutagenesis—Mutagenesis (C1093A) of the recombinant human TRPM4 cDNA in the pcDNA4/TO vector was performed using the QuikChange site-directed mutagenesis kit (Stratagene, La Jolla, CA) as per the manufacturer's instructions, using the primers: forward, 5′-TGCTCAG-GCAATTGGCTAGGCGACC-3′ and reverse, 5′-GGTCGC-CTAGCCAATTGCCTGAGCA-3′. The nucleotide sequence of the mutant was verified by DNA sequencing.

Electrophysiology—Whole cell patch clamp experiments on T-REx-293 hTRPM4 cells were performed 16–24 h after tetracycline induction. In acute overexpression experiments, HEK 293 cells were transfected with the plasmid containing the C1093A mutation using Lipofectamine 2000 and electrophysiological experiments were conducted 48 h post transfection. For whole cell experiments, the internal pipette solution contained (in mM) CsCl 140, NaCl 5, $MgCl_2$ 1, BAPTA 1, $CaCl_2$ 0.83, and pH 7.2 adjusted with CsOH. The bath solution (in mM) was: NaCl 140, CsCl 5, $CaCl_2$ 1, $MgCl_2$ 1, glucose 10, HEPES 10, tamoxifen 0.01, and pH 7.4 adjusted with NaOH. For current clamp experiments, the pipette solution contained (in mM): KCl 140, NaCl 5, HEPES 10, $CaCl_2$ 0.01, $MgCl_2$ 1, pH 7.2, adjusted with KOH and the bath solution contained (in mM), NaCl 140, KCl 5, $CaCl_2$ 1, $MgCl_2$ 1, glucose 10, HEPES, 10, tamoxifen, 0.01, and pH was adjusted to 7.4 with NaOH. In inside-out experiments, the pipette solution contained (in mM): 140 NaCl, 5 KCl, 1 $MgCl_2$, 1 $CaCl_2$, 10 HEPES, pH 7.4, adjusted with KOH. The bath solution contained (in mM): 140 NaCl, 5 KCl, 1 $MgCl_2$, 0.01 $CaCl_2$, 10 HEPES, 1 HEDTA, pH 7.2, adjusted with NaOH. Free $[Ca^{2+}]$ of the solutions was calculated using the program WinMaxc, version 2.50 with the appropriate Ca^{2+} buffers. Patch clamp experiments were performed using an Axopatch 200B amplifier (Molecular Devices Corp., Sunnyvale, CA). Data were digitized at 10 kHz and low-pass filtered at 1 kHz. The pClamp 9.2 software (Molecular Devices Corp.) was used for data acquisition and analysis. Patch electrodes (~3 MΩ resistance) were pulled from borosilicate glass (Warner Instruments, Hamden, CT) using a BB-CH puller (Mecanex SA, Geneva, Switzerland). When applicable, voltages were corrected for liquid junction potentials. All experiments were conducted at 22 ± 2 °C.

Cell Death Determination by LDH Release—T-REx-293 hTRPM4 cells were exposed to experimental conditions in DMEM/F-12 supplemented with 1% bovine serum albumin instead of FBS. Cells were exposed to H_2O_2 (Merck KgaA-Chemicals, Darmstad, Germany) for 4 h and viability was determined 20 h later. Lactate dehydrogenase (LDH) activity in cell supernatants was determined by a colorimetric end point kit according to the manufacturer's instructions (Roche Applied Science). A calibration curve was produced to ensure linearity in the range studied. Background was subtracted and data were expressed as the fraction of maximum release measured in the presence of 1% Triton X-100 (Sigma).

Cell Death Determination by FACS—T-REx-293 hTRPM4 or HeLa cells were exposed to experimental conditions in DMEM/F-12 or DMEM-low glucose, respectively, supplemented with 1% bovine serum albumin instead of FBS. Cells were exposed to H_2O_2 for 4 h and viability was determined 20 h later. In selected experiments, DMEM was made following the manufacturer's instructions (Invitrogen) and reagents to facilitate Na^+ replacement. HEPES (25 mM) was used as a buffer instead of $NaHCO_3$ and cells were kept at 37 °C without CO_2. Sodium was replaced equimolarly by *N*-methyl-D-glucamine or sucrose. Osmolarity was kept constant across different solutions. Osmolarity was measured with a micro-osmometer (Advanced Instruments, Norwood, MA). Cells were harvested by centrifugation at 800 $\times$ *g* for 5 min and the pellet was suspended in 200 μl of PBS. Afterward, cells were washed once with PBS and stained with propidium iodide (PI, 10 μg/ml, Sigma) for 20 min at room temperature in the dark. DNA content was analyzed with a flow cytometry system (FACSCanto, BD Biosciences). A minimum
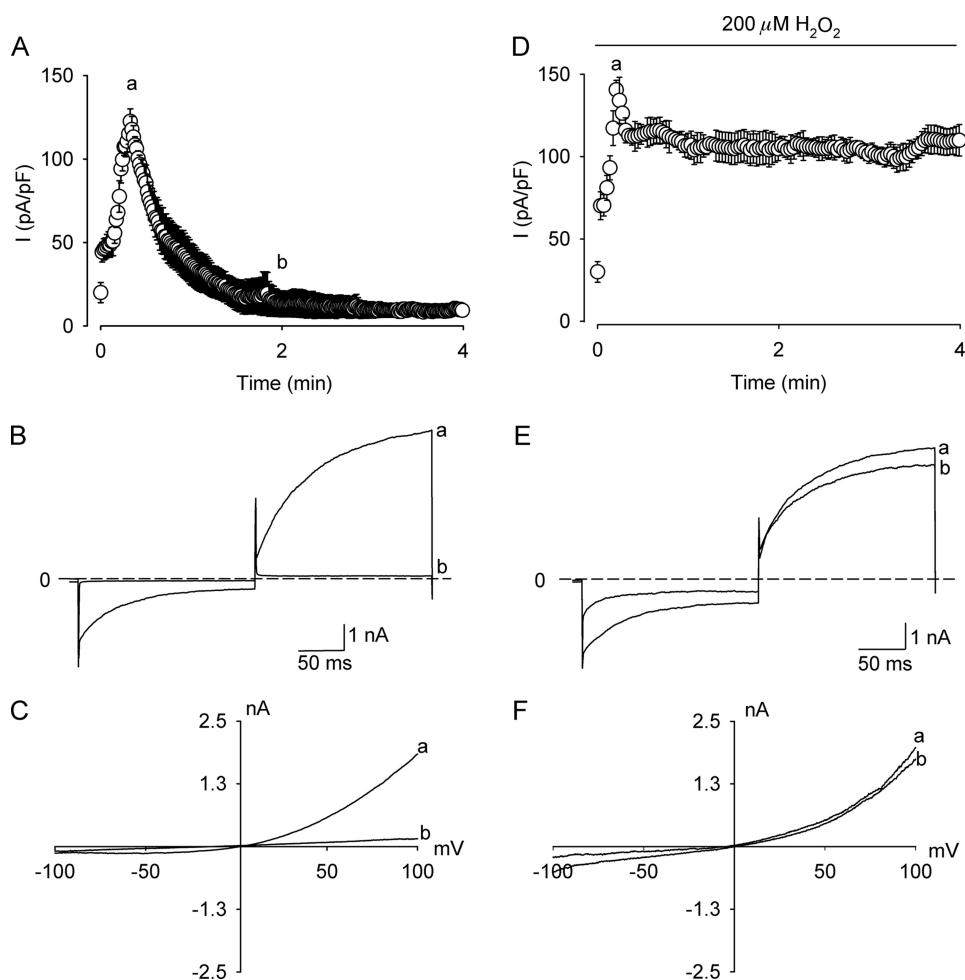
FIGURE 1. **H$_2$O$_2$ removes desensitization of TRPM4 currents.** *A*, time course of averaged (mean $\pm$ S.E., *n* = 10) TRPM4 currents recorded at 100 mV evoked by 600 nM Ca^{2+} in the pipette solution from tetracycline-induced (1 μg/ml) (HEK-TRPM4 *tet*+) cells. The voltage protocol consisted in a 400-ms step to -100 mV from a holding potential of 0 mV followed by a 400-ms step to 100 mV applied at 0.4 Hz (only positive currents are shown). The depicted current corresponds to the mean current recorded during the 20-ms final pulse. *B*, representative whole cell current traces at -100 and 100 mV obtained with the same protocol as described above. *C*, representative *I-V* relationship of TRPM4 currents using a voltage ramp from -100 to 120 mV. The ramp protocol consisted of an 800-ms ramp from -100 to 120 mV from a holding potential of 0 mV. *D*, time course of averaged (mean $\pm$ S.E., *n* = 8) TRPM4 currents from HEK-TRPM4 *tet*+ cells exposed to 200 μM H$_2$O$_2$ recorded at 100 mV with 600 nM Ca^{2+} in the pipette solution. *E*, representative whole cell current traces from HEK-TRPM4 *tet*+ cells exposed to 200 μM H$_2$O$_2$ and dialyzed with 600 nM Ca^{2+}. *F*, representative *I-V* relationship as in *B* from HEK-TRPM4 *tet*+ cells challenged with 200 μM H$_2$O$_2$. In all panels, *a* indicates the peak currents (30 s after establishing the whole-cell configuration) and *b* denotes the current after 120 s of cell dialysis.

of 10,000 cells/sample were analyzed. PI intensity analysis was performed using FACSDiva software version 4.1.1 (BD Biosciences). Cell death was determined according to a previously described method (26). In brief, PI enters the cell upon plasma membrane disruption thus binding to DNA. Because its fluorescence is proportional to the DNA content, live cells (M$_0$) present a low fluorescence, whereas in necrotic cells (M$_2$) PI binds mainly to intact DNA showing a high fluorescence. Apoptotic cells with degraded DNA (M$_1$) bind less PI than necrotic cells but its fluorescence is higher than M$_0$.

Cell Volume Measurements—shRNA-TRPM4 and shRNA-SS HeLa cells cultured on 25-mm glass coverslips were put into a recording chamber mounted on a confocal spinning disk system (DSU Olympus, Germany) and changes in cell water volume of individual cells were assessed by measuring variations in the concentration of the intracellularly trapped fluorescent dye

red calcein (Invitrogen), with an excitation wavelength of 555 nm and emission wavelength between 580 and 620 nm recorded with a band pass filter, similar as previously described (27, 28). Briefly, cells were loaded with 5 μM calcein-AM for 5 min and then superfused with an isosmotic solution for 15 min before adding H$_2$O$_2$. Images were obtained at 10-s intervals and the fluorescence of a ~10-μm^2 area in the center of a cell was measured. Data are presented as V_t/V_0 values, where V_0 is the cell water volume in isosmotic solution at time 0 and V_t is the cell water volume at time *t*. V_t/V_0 was calculated from the fluorescence intensity ratio F_0/F_t.

Immunoblot Analysis—Cells were harvested and collected by centrifugation (3,000 $\times$ *g* at 4 °C) and lysed in a lysis buffer (1% Triton X-100, 150 mM NaCl, 1 mM EDTA, 50 mM Tris-HCl, 1 mM sodium orthovanadate, 5 mM NaF, 1 mM PMSF, 1.5 μg/ml of aprotinin, 10 μg/ml of antipain, 10 μg/ml of leupeptin, 0.1 mg/ml of benzamidine, pH 7.4). Lysates were centrifuged at 12,000 $\times$ *g* for 10 min at 4 °C and proteins from the supernatants were size-fractionated in 6 and 12% SDS-PAGE (29) and transferred to nitrocellulose membranes for Western blot analysis with anti-FLAG and anti-β-actin polyclonal antibodies (Sigma), respectively.

Reagents—Unless stated, all chemicals and reagents were from Merck KgaA-Chemicals (Darmstad, Germany) and Sigma.

Data Analysis—All results are presented as mean $\pm$ S.E. from 3 or more independent experiments. Statistical analysis of the data were performed using Statgraphics Plus 5.0 (GraphPad Software, Inc., San Diego, CA). ANOVA followed by the Bonferroni or Dunns post hoc tests and Student's *t* test were used and considered significant at *p* < 0.05.

RESULTS

Hydrogen Peroxide Removes TRPM4 Desensitization in a Heterologous Overexpression Model—To address the role of TRPM4 in ROS-mediated cell death, we first explored whether TRPM4 would be sensitive to ROS. Fig. 1*A* shows an averaged time course of currents measured at 100 mV activated by 600 nM Ca^{2+} in the pipette solution in T-REx-293 hTRPM4 cells overexpressing TRPM4 under the control of a *tet* inducible system (HEK-TRPM4 *tet*+) (24) (supplemental Fig. S1*A*). As

expected for heterologously overexpressed TRPM4 channels, the current was transient and appeared to be completely abolished after 2 min and showed no reactivation even at 20 min (supplemental Fig. S1*B*) (7, 30). To discard that the recorded current was carried by Cl⁻ ions, experiments were performed in which the extracellular NaCl concentration was reduced to 40 mM. As predictable for a cation current, the reversal potential shifted to −31 mV, close to the expected value of −29 mV (*n* = 8). There was no influence of H₂O₂ on the reversal potential of the currents. Fig. 1*B* depicts representative control whole cell current traces at −100 and 100 mV recorded at 30 (peak) and 120 s after breaking into the cell. The *I-V* curves obtained from representative voltage ramps, measured at the peak and 120 s, display the typical rectification found for TRPM4 currents (Fig. 1*C*) (4). To study the effect of H₂O₂ on TRPM4 currents, HEK-TRPM4 *tet+* cells were exposed to 200 μM H₂O₂ throughout the recording. In the experiments with H₂O₂, tamoxifen was used to avoid contamination with volume-activated Cl⁻ currents (31). As depicted in Fig. 1*D*, the current (measured at 100 mV) remained activated and showed very little desensitization. The loss of desensitization was also evident when observing traces recorded at −100 and 100 mV (Fig. 1*E*). The *I-V* relationship was comparable with control conditions at the peak and at later times during the experiment, yet showed less inward rectification (Fig. 1*F*). The effect of H₂O₂ was dose-dependent and became apparent at concentrations ≥50 μM without significant modification of the voltage dependence (supplemental Fig. 1, *C* and *D*). The effect of H₂O₂ on TRPM4 currents was also observed in whole cell (supplemental Fig. S1*E*) and inside-out recordings (supplemental Fig. S1*F*) upon exposure to H₂O₂ after current desensitization. Flufenamic acid (100 μM) or glibenclamide (10 μM), two known inhibitors of TRPM4 (32) significantly reduced this non-desensitizing current from 148 ± 15.8 to 5 ± 2.1 and 9.6 ± 5.6 pA/pF, respectively (not shown).

The Cys¹⁰⁹³ Residue Participates in Mediating the Effect of H₂O₂—Because of the striking similarity between the effect of H₂O₂ and an increased calmodulin binding at the C terminus region on whole cell current desensitization (30), we focused our interest in the cysteine residue located at position 1093 in the C terminus next to the beginning of the third CaM binding motif spanning the Arg¹⁰⁹⁵-Thr¹¹⁵¹ sequence (30). It should be noted that no cysteine residues were found close to the other predicted CaM binding motif located at the C terminus of the protein. To that end, this cysteine residue was mutated to alanine and the effect of H₂O₂ on HEK 293 cells overexpressing the mutation was explored electrophysiologically. Fig. 2*A* shows a representative time course experiment of whole cell currents measured at 100 mV activated by 600 nM Ca²⁺ in the pipette solution. In contrast to wild type TRPM4 currents (Fig. 1*D*), exposure to 200 μM H₂O₂ had no effect on current desensitization, suggesting that for H₂O₂ to be effective requires the Cys¹⁰⁹³ residue. Because of the complexity of the processes and the variety of factors that apparently govern the desensitization of TRPM4 currents, we next asked the question whether the rescue from desensitization by PI(4,5)P₂ of this mutant was hindered. Fig. 2 depicts representative time course experiments of inside-out patches from HEK 293 cells overexpressing wild type
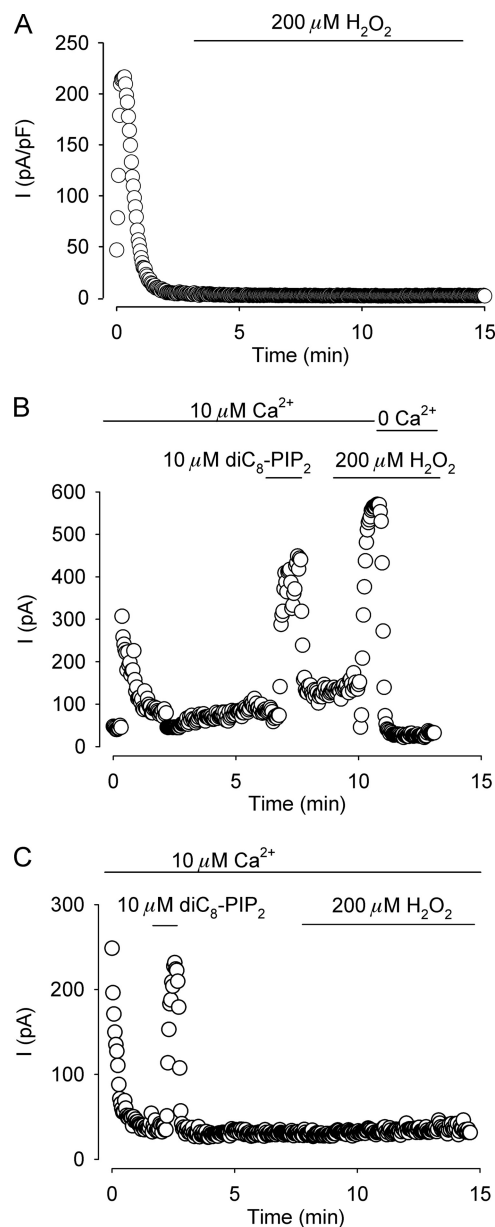

FIGURE 2. **C1093A mutant channels do not respond to H₂O₂.** *A*, representative time course of TRPM4 whole cell currents from HEK 293 cells overexpressing the C1093A mutant exposed to 200 μM H₂O₂ (indicated by the *bar*) recorded at 100 mV with 600 nM Ca²⁺ in the pipette solution (*n* = 12). *B* and *C*, representative time course of inside-out recordings from membrane patches from HEK 293 cells overexpressing wild type TRPM4 channels (*B*) or C1093A mutants (*C*) recorded at 100 mV and activated by 10 μM Ca²⁺ in the bath solution. *Bars* indicate exposure to the water-soluble form of PI(4,5)P₂ (dioctanoyl-phosphatidylinositol-4,5-bisphosphate (*diC₈-PIP₂*), Echelon Biosciences Inc., Salt Lake City, UT) or 200 μM H₂O₂ (*n* = 10 for wild type TRPM4 channels and *n* = 12 for C1093A mutants).

TRPM4 channels (B) or channels carrying the C1093A mutation (C). The current was activated in the presence of 10 μM Ca²⁺ in the bath solution and recorded at 100 mV. As shown, the C1093A mutant retains the sensitivity to PI(4,5)P₂, indicating that H₂O₂ does not hamper the action of PI(4,5)P₂.

Overexpression of TRPM4 Increases H₂O₂-dependent Cell Death—To study whether a persistent, non-desensitizing TRPM4-mediated current would have an impact on cell viability, we measured LDH release of HEK-TRPM4 *tet+* cells sub-
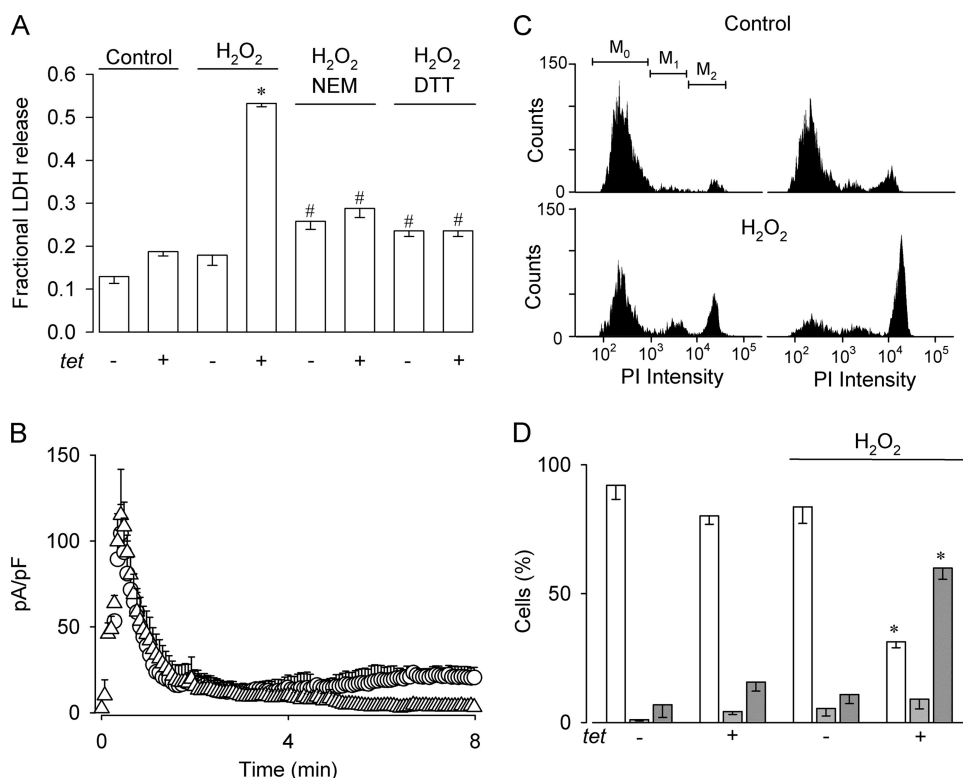
FIGURE 3. **Heterologous TRPM4 expression renders HEK 293 cells vulnerable to H₂O₂-induced cell death.** *A*, *bars* show the fraction of LDH released (mean ± S.E., *n* = 3) comparing HEK-TRPM4 *tet+* and HEK-TRPM4 *tet−* cells in the absence or presence of 200 μM H₂O₂, as well as cells exposed to H₂O₂ preincubated with 5 mM NEM by 1 h or 5 mM DTT by 3 h. Statistical differences were assessed by ANOVA and Dunns post hoc tests, *, *p* < 0.05 compared with control conditions, #, *p* < 0.05 compared with *tet+* plus H₂O₂. *B*, averaged (mean ± S.E., *n* = 4 for each condition) time course of TRPM4 whole cell currents recorded at 100 mV in HEK-TRPM4 *tet+* cells with 600 nM Ca²⁺ in the pipette solution preincubated with 200 μM NEM for 10 min (△) and 200 μM NEM for 10 min followed with an exposure to 200 μM H₂O₂ (○). Voltage protocol as described in the legend to Fig. 1*A*. *C*, representative PI incorporation histograms of HEK-TRPM4 *tet−* (*top panel*, *left*) and HEK-TRPM4 *tet+* cells (*top panel*, *right*) under control conditions (control) and in the presence of 200 μM H₂O₂ (H₂O₂) (*bottom panels*, *left* and *right*, respectively). Cells were analyzed by FACS and markers M_0, M_1, and M_2 indicate live, apoptotic, and necrotic cell populations, respectively. *D*, *bars* show the percentage (mean ± S.E.) of live (*empty bars*), apoptotic (*light gray bars*), and necrotic (*dark gray bars*) cells from HEK-TRPM4 *tet+* and HEK-TRPM4 *tet−* cells in the absence or presence of 200 μM H₂O₂ for 4 h; *n* = 5 independent experiments as those depicted in *C*. Cell populations were determined by PI incorporation measured 20 h after the removal of H₂O₂. Statistical differences were assessed by ANOVA and Bonferroni post hoc tests, *, *p* < 0.05 against either live or necrotic populations.
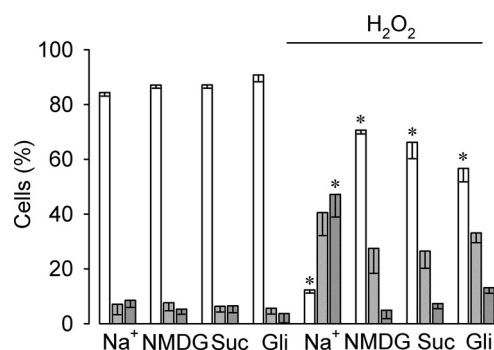
FIGURE 4. **Effect of extracellular Na⁺ and glibenclamide on H₂O₂-induced cell death in HeLa cells.** *Bars* show the percentage (mean ± S.E., *n* = 3) of live (*empty bars*), apoptotic (*light gray bars*), and necrotic (*dark gray bars*) HeLa wild type cells in the absence or presence of 1 mM H₂O₂ for 4 h. Cells were cultured in DMEM with normal extracellular NaCl or modified DMEM (Na⁺-free) in which NaCl was replaced with *N*-methyl-D-glucamine (*NMDG*)-Cl or sucrose (*suc*). For the glibenclamide experiments, the drug (100 μM) was added to the medium 1 h before H₂O₂ addition and maintained throughout the entire experiment. Cell populations were determined by PI incorporation and measured 20 h after H₂O₂ removal. Statistical differences were assessed by ANOVA and Dunns post hoc tests, *, *p* < 0.05 against either live or necrotic populations.

jected to H₂O₂. To that purpose, cells were incubated with 200 μM H₂O₂ for 4 h and LDH release was assessed 20 h after H₂O₂ removal. As seen in Fig. 3*A*, H₂O₂ did not alter significantly the proportion of live cells in HEK-TRPM4 *tet−* cells. In contrast, HEK-TRPM4 *tet+* cells exhibited a significant increase in cell death that was reduced by preincubation with NEM or DTT. As shown in Fig. 3*B*, the effect of NEM on cell death was correlated with the inhibition by NEM of the effect of H₂O₂ on TRPM4 currents. The thiol-alkylating agent NEM was used to prevent H₂O₂-mediated oxidation of cysteine residues. On the other hand, DTT was used to block H₂O₂-induced thiol modifications, maintaining these groups in a reduced state. To characterize further the H₂O₂-mediated cell death, flow cytometer experiments were performed. Fig. 3*C* displays representative histograms of PI incorporation for untreated HEK-TRPM4 *tet−* and HEK-TRPM4 *tet+* cells and cells were exposed to 200 μM H₂O₂ using the same protocol as described for the LDH release experiments. As shown, H₂O₂ induced an increase in the M_2 population (~5.5-fold) corresponding to necrotic cells along with a decrease in the M_0 population (~2.7-fold), corresponding to live cells, both compared with untreated HEK-TRPM4 *tet−* and HEK-TRPM4 *tet+* cells (Fig. 3*D*). However, the proportion of apoptotic cells (M_1) was not affected by H₂O₂.

H₂O₂-induced Cell Death in HeLa Cells—Next, we explored whether native TRPM4 might play a role in H₂O₂-induced epithelial cell necrosis. Because TRPM4 mRNA has been detected in several cell lines, including HeLa cells (33), we used these cells as a model. To address this issue we performed extracellular cation replacement experiments and evaluated cell viability with flow cytometry upon exposure to H₂O₂. In contrast to HEK-TRPM4 *tet+* cells, HeLa cells appeared to be more resistant to H₂O₂ and thus, cell death was detected at concentrations ≥0.8 mM (not shown). As depicted in Fig. 4, a 4-h long exposure to 1 mM H₂O₂ in the presence of extracellular Na⁺ triggered a ~7-fold decrease in viable cells, a ~5.7-fold increase in apoptotic cells, and a ~9-fold increase in the necrotic population. Extracellular Na⁺ replacement by the impermeant cation *N*-methyl-D-glucamine or sucrose during H₂O₂ exposure reduced the necrotic (M_2) population to control values, yet the apoptotic (M_1) population did not differ significantly from that observed under conditions of normal extracellular Na⁺. In line
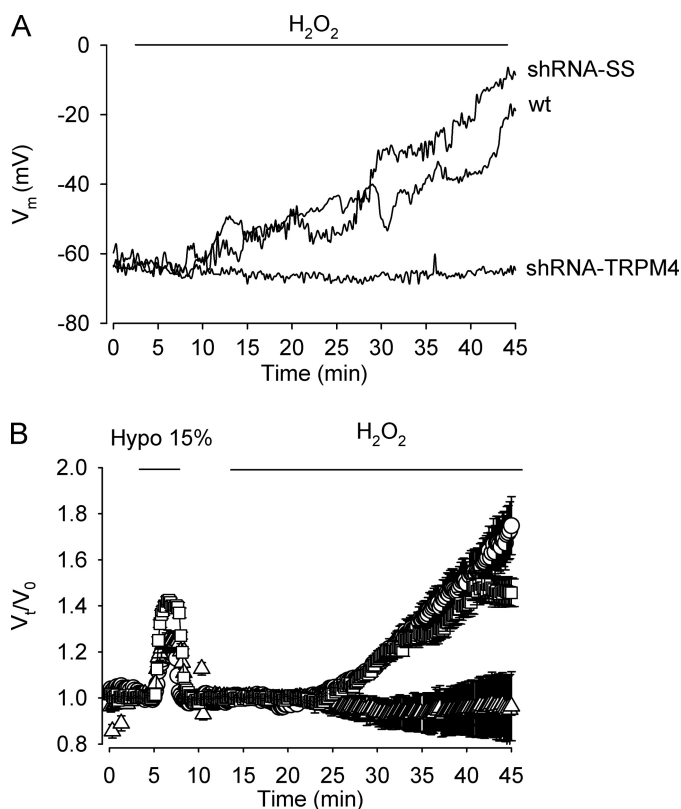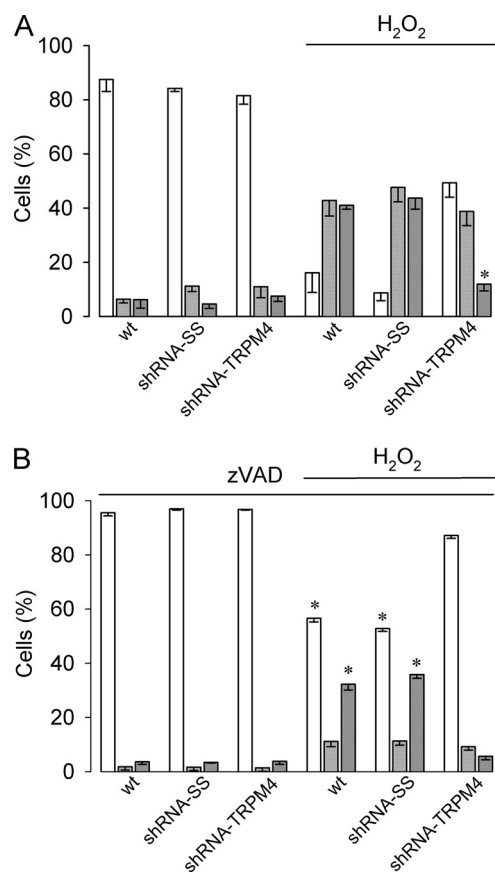
FIGURE 5. **TRPM4 participates in H$_2$O$_2$-induced cell depolarization and volume increase.** *A*, representative current clamp recording of WT, shRNA-SS, and shRNA-TRPM4 HeLa cells exposed to 1 mM H$_2$O$_2$. *B*, experiments showing the effect of 1 mM H$_2$O$_2$ on cell volume in shRNA-SS HeLa cells (*circles*), shRNA-TRPM4 HeLa cells (*triangles*), and WT HeLa cells (*squares*). For calibration purposes, cells were briefly exposed to a 15% hypotonic solution. Each point represents the mean ± S.E. of values obtained from 12 to 15 cells (*n* = 4 independent experiments).

FIGURE 6. **Interference RNA against TRPM4 protects HeLa cells from H$_2$O$_2$-induced necrotic cell death.** *A*, bars show the percentage (mean ± S.E., *n* = 9) of live (*empty bars*), apoptotic (*light gray bars*), and necrotic (*dark gray bars*) cells from wild type HeLa cells and HeLa cell clones stably expressing shRNA-SS (*shRNA-SS*) and shRNA-TRPM4 (*shRNA-TRPM4*) cultured in the absence or presence of 1 mM H$_2$O$_2$ for 4 h. Cell populations were determined by PI incorporation and measured 20 h after H$_2$O$_2$ removal. Statistical differences were assessed by ANOVA and Bonferroni post hoc tests, *, *p* < 0.05 indicates a significant change respect to necrosis in wild type (*wt*) and TRPM4-SS (*TRPM4-SS*) cells in the presence of H$_2$O$_2$. *B*, same experiment described in *A* except that cells were preincubated (1 h) and maintained throughout with Z-VAD (10 μM), mean ± S.E., *n* = 6. Statistical differences were assessed by ANOVA and Bonferroni post hoc tests, *, *p* < 0.05 against either live or necrotic populations.

with these results, the unspecific TRPM4 blocker glibenclamide decreased H$_2$O$_2$-induced necrotic cell death.

TRPM4 Is Important for H$_2$O$_2$-induced Necrosis in HeLa Cells—Because of the lack of specific pharmacological tools available to block TRPM4 as well as to rule out the participation of other ROS-sensitive TRPM4-related channels, such as TRPM2 and TRPM7 in H$_2$O$_2$-induced necrosis in HeLa cells, the participation of endogenous TRPM4 channels in cell death was explored by knocking down the expression of TRPM4 with RNAi tools. For that purpose, HeLa cell lines stably expressing a shRNA against TRPM4 (shRNA-TRPM4) or a scramble sequence (shRNA-SS) (24) were generated. To test the efficiency and specificity of the shRNA, we conducted qPCR experiments. As shown in supplemental Fig. S2, expression of TRPM4 was reduced by ~80% in shRNA-TRPM4 cells compared with cells transfected with shRNA-SS. Additionally, shRNA-TRPM4 proved to be specific for TRPM4 as observed by the lack of effect on TRPM2 and TRPM7 transcripts.

Given that a persistent activity of nonselective cation channels would eventually reduce membrane potential, we studied the effect of H$_2$O$_2$ on the membrane potential in HeLa cells. To that end, current clamp recordings were performed. As illustrated in Fig. 5*A*, the resting membrane potential of wild type, shRNA-SS, and shRNA-TRPM4 HeLa cells under basal conditions were similar, however, upon continuous exposure to 1 mM

H$_2$O$_2$, shRNA-SS HeLa cells as well as wild type HeLa cells gradually depolarized reaching values close to 0 mV. In contrast, shRNA-TRPM4 HeLa cells maintained their resting membrane potential. The progressive collapse of the membrane potential observed in wild type and shRNA-SS HeLa cells exposed to H$_2$O$_2$ was paralleled by a significant increase in cell volume (Fig. 5*B*). Loss of membrane potential and thus, normal ion gradients would have a profound impact on cell function, particularly cell viability. Therefore, if TRPM4 plays a role in H$_2$O$_2$-induced necrosis, it can be anticipated that shRNA-TRPM4 HeLa cells would become relatively resistant to H$_2$O$_2$. As shown in Fig. 6*A*, necrosis was significantly (~3.6-fold) reduced in shRNA-TRPM4 cells compared with wild type or shRNA-SS cells and not significantly different from necrosis detected in untreated shRNA-TRPM4 cells. In contrast, H$_2$O$_2$-induced apoptosis remained unaffected in shRNA-TRPM4 cells. To define whether the reduction in cell viability observed after H$_2$O$_2$ exposure is caspase-dependent, a generic caspase inhibitor was used. As depicted in Fig. 6*B*, the pan-caspase

A

B
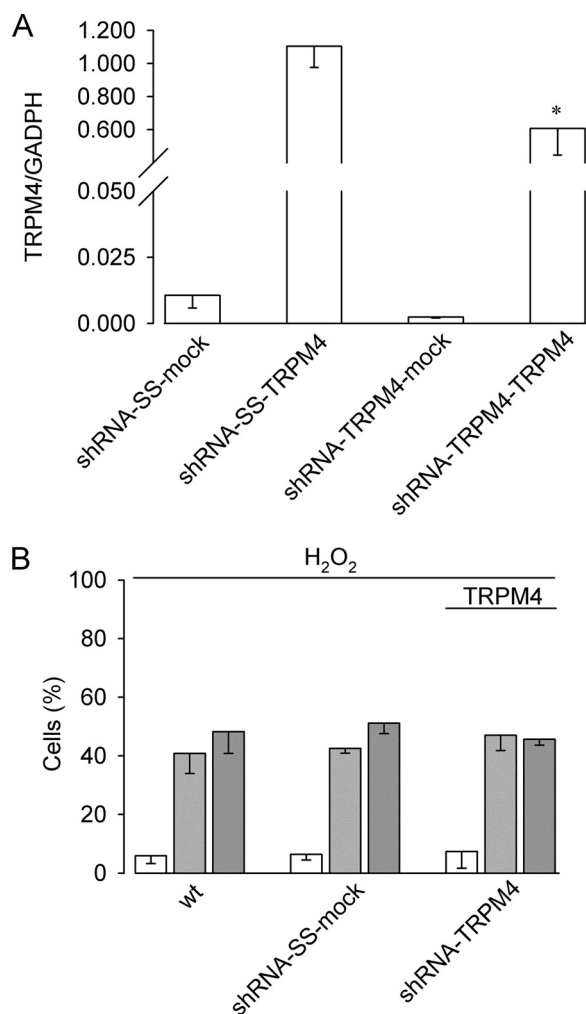
FIGURE 7. **TRPM4 re-expression in TRPM4-deficient HeLa cells re-establishes H$_2$O$_2$-induced necrosis.** *A*, real time quantitative PCR analysis (mean ± S.E., $n = 3$) of HeLa cell clones stably expressing shRNA-SS or shRNA-TRPM4 transfected with an empty vector (*shRNA-SS-mock* and *shRNA-TRPM4-mock*) or the pcDNA4/TO-TRPM4 expression plasmid (*shRNA-SS-TRPM4* or *shRNA-TRPM4-TRPM4*). Data are expressed as relative levels to GADPH transcript. Statistical differences were assessed by Student's *t* test, *, $p < 0.05$. *B*, bars show the percentage (mean ± S.E., $n = 4$) of live (*empty bars*), apoptotic (*light gray bars*), and necrotic (*dark gray bars*) of wt HeLa cells, shRNA-SS (*shRNA-SS-mock*) and shRNA-TRPM4 (*shRNA-TRPM4*) HeLa cell clones cultured in the presence of 1 mM H$_2$O$_2$ for 4 h. shRNA cells were transfected with the pcDNA4/TO-TRPM4 expression plasmid 48 h before the experiment.

inhibitor Z-VAD exerted its effect by mainly reducing H$_2$O$_2$-induced apoptosis in wild type and shRNA-SS cells. However, in shRNA-TRPM4 cells, Z-VAD was protected from H$_2$O$_2$-induced apoptosis and, to a lesser extent necrosis.

Re-expression of TRPM4 Sensitizes HeLa Cells to H$_2$O$_2$-induced Necrosis—To prove that TRPM4 expression is sufficient to sustain H$_2$O$_2$-induced necrosis in HeLa cells and to discard siRNA off-target effects, shRNA-TRPM4, shRNA-SS, and wild type HeLa cells were acutely transfected with a cDNA-hTRPM4 expression plasmid or mock transfected with an empty plasmid. Because we used a non-mutated hTRPM4 cDNA, we determined first the efficiency of re-expression of the mRNA. As shown in Fig. 7A, acute transfection of the hTRPM4-containing plasmid into shRNA-TRPM4 HeLa cells restored ~60% TRPM4 mRNA levels compared with shRNA-SS acutely transfected with the hTRPM4 plasmid. We
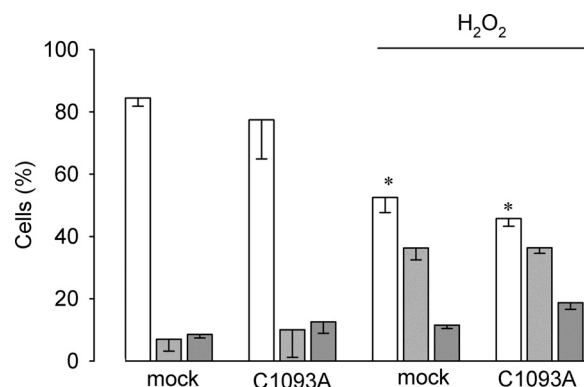
FIGURE 8. **TRPM4-C1093A expression in TRPM4-deficient HeLa cells does not re-establish H$_2$O$_2$-induced necrosis.** shRNA-TRPM4 cells were transiently transfected with empty plasmid (*mock*) or a plasmid containing the mutated (C1093A) version of TRPM4. Cells were cultured in the absence or presence of 1 mM H$_2$O$_2$ for 4 h. *Bars* show the percentage (mean ± S.E., $n = 4$) of live (*empty bars*), apoptotic (*light gray bars*), and necrotic (*dark gray bars*). Statistical differences were assessed by ANOVA, *, < 0.05 against either live or necrotic populations.

next exposed the cells to H$_2$O$_2$ and measured PI incorporation. As seen in Fig. 7B, shRNA-TRPM4 cells transfected with TRPM4 were found to be as sensitive as wild type and shRNA-SS cells to H$_2$O$_2$-induced necrosis.

Finally, we tested whether shRNA-TRPM4 HeLa cells transfected with a plasmid encoding the C1093A mutation would remain insensitive to H$_2$O$_2$-induced necrotic cell death. As depicted in Fig. 8 transient transfection of shRNA-TRPM4 cells with the mutated TRPM4 did not restore vulnerability to H$_2$O$_2$-induced necrotic cell death.

DISCUSSION

Necrosis is hallmarked by a non-compensated increase in cell volume, in part due to unregulated osmotically driven water flux. Although several studies have shown that Na$^+$ permeability is increased in various cell types under oxidative stress, the molecular identity of the channel(s) responsible remain unknown. In the present work we show that H$_2$O$_2$-induced necrotic cell death in HEK 293 and HeLa cells is dependent on the expression and activity of TRPM4. The experiments reported here indicate that H$_2$O$_2$ abolishes, in a concentration-dependent manner, the desensitization usually observed for heterologously expressed TRPM4 channels, giving rise to a sustained current.

The effect of H$_2$O$_2$ on TRPM4 was prevented by DTT and thiol-alkylating agents, suggesting the involvement of cysteine residues in this phenomenon. Reversible oxidation of cysteine side chains to sulfenic acid (Cys-SOH) and its wide ranging biological relevance has come into view during the last decade (34) (for review, see Ref. 35). Using functional site profiling and electrostatic analysis, Salsbury *et al.* (36) identified common features found in redox-sensitive cysteine residues. We hypothesized that Cys[1093] could be a putative redox-modifiable cysteine residue due to its close proximity to a proline residue (Pro[1096]) and several arginine residues (Arg[1090], Arg[1094], and Arg[1095]) that may lower the pK_a of Cys[1093], enhancing its reactivity to ROS (36). As reported here, H$_2$O$_2$ specifically modulates channel desensitization, yet does not affect channel activation as the sustained current induced by H$_2$O$_2$ remains

strictly dependent on Ca^{2+}. TRPM4 desensitization has been related to $PI(4,5)P_2$ depletion (7). Our results show that $PI(4,5)P_2$ is able to rescue from desensitization both the wild type TRPM4, as well as the C1093A mutated TRPM4 channels, suggesting that the effect of H_2O_2 is likely to be independent of $PI(4,5)P_2$. Although a definitive demonstration of the mechanisms for H_2O_2 action remains to be settled, a plausible interpretation of our data is that redox modifications of this residue could increase CaM binding to the channel, therefore reducing current desensitization.

The involvement of TRP channels in hypoxia/reperfusion-mediated damage is not without precedent. In smooth muscle cells of the pulmonary artery, hypoxia has been shown to augment several times TRPC1 and TRPC6 mRNA and protein levels (37, 38). Increased oxidative stress levels are associated with reperfusion and evidence suggests that Ca^{2+} influx via redox-modulated TRP channels is a relevant mechanism through which oxidative stress mediates cell death. TRPM7, a member of the TRPM subfamily, was associated with oxygen glucose deprivation currents in cortical neurons and its suppression prevented anoxic death (39). Furthermore, TRPM2 was found to be activated by micromolar levels of H_2O_2 through a cADPR-dependent mechanism (40, 41). In contrast to TRPM2 and TRPM7, which are ROS-sensitive and known to participate in cell death, TRPM4 is Ca^{2+}-impermeant cation channel and thus, its effects on cell death cannot be simply explained by Ca^{2+} influx and subsequent intracellular Ca^{2+} overload. Of note, overexpression of TRPM4 in COS-7 cells was found to render these cells susceptible to oncotic cell death in the absence of ATP (21), a phenomenon that could be additionally explained in view of our results by the direct effect of H_2O_2 on TRPM4 activity.

The effect of H_2O_2 on TRPM4 currents was accompanied with a substantial increase mainly in H_2O_2-mediated necrosis in HEK 293 cells. At variance, H_2O_2 induced both apoptosis and necrosis cell death in HeLa cells that endogenously express TRPM4 and exhibited both, apoptosis and necrosis. However, only necrosis was found to be dependent on the extracellular cation. Sodium removal and replacement with non-permeant cations significantly decreased necrosis, suggesting that intracellular Na^+ overload and thus, cell volume increase is an important factor for H_2O_2-induced necrosis in HeLa cells. In line with this finding, H_2O_2-induced necrosis but not apoptosis was prevented in HeLa cells stably expressing a shRNA against TRPM4. Of note, the generic caspase inhibitor Z-VAD in addition to reducing apoptosis, also decreased H_2O_2-induced necrosis in shRNA-TRPM4 cells, reflecting a caspase-dependent component of necrosis (42). Consistent with a sustained activity of a non-selective cation channel, H_2O_2 induced a significant cell depolarization in both wild type and shRNA-SS HeLa cells, whereas shRNA-TRPM4 HeLa cells maintained a normal resting potential. Thus, we propose that prolonged activity of TRPM4 channels plays a significant role in oxidative stress-mediated changes of membrane potential and transmembrane ionic gradients contributing to necrotic cell death.

REFERENCES

1. Venkatachalam, K., and Montell, C. (2007) *Annu. Rev. Biochem.* **76,** 387–417
2. Miller, B. A. (2006) *J. Membr. Biol.* **209,** 31–41
3. Launay, P., Fleig, A., Perraud, A. L., Scharenberg, A. M., Penner, R., and Kinet, J. P. (2002) *Cell* **109,** 397–407
4. Nilius, B., Prenen, J., Droogmans, G., Voets, T., Vennekens, R., Freichel, M., Wissenbach, U., and Flockerzi, V. (2003) *J. Biol. Chem.* **278,** 30813–30820
5. Nilius, B., Prenen, J., Voets, T., and Droogmans, G. (2004) *Pflügers Arch.* **448,** 70–75
6. Hofmann, T., Chubanov, V., Gudermann, T., and Montell, C. (2003) *Curr. Biol.* **13,** 1153–1158
7. Zhang, Z., Okawa, H., Wang, Y., and Liman, E. R. (2005) *J. Biol. Chem.* **280,** 39185–39192
8. Nilius, B., Mahieu, F., Prenen, J., Janssens, A., Owsianik, G., Vennekens, R., and Voets, T. (2006) *EMBO J.* **25,** 467–478
9. Chen, M., and Simard, J. M. (2001) *J. Neurosci.* **21,** 6512–6521
10. Petersen, O. H. (2002) *Curr. Biol.* **12,** R520–R522
11. Inoue, M., Fujishiro, N., and Imanaga, I. (1999) *J. Physiol.* **519,** 385–396
12. Schlenker, T., Feranchak, A. P., Schwake, L., Stremmel, W., Roman, R. M., and Fitz, J. G. (2000) *Gastroenterology* **118,** 395–403
13. Koliwad, S. K., Kunze, D. L., and Elliott, S. J. (1996) *J. Physiol.* **491,** 1–12
14. Herson, P. S., and Ashford, M. L. (1997) *J. Physiol.* **501,** 59–66
15. Barros, L. F., Stutzin, A., Calixto, A., Catalán, M., Castro, J., Hetz, C., and Hermosilla, T. (2001) *Hepatology* **33,** 114–122
16. Jeulin, C., Dazy, A. C., and Marano, F. (2002) *Pflügers Arch.* **443,** 574–583
17. Simon, F., Varela, D., Eguiguren, A. L., Díaz, L. F., Sala, F., and Stutzin, A. (2004) *Am. J. Physiol. Cell Physiol.* **287,** C963–C970
18. Barros, L. F., Hermosilla, T., and Castro, J. (2001) *Comp. Biochem. Physiol. A Mol. Integr. Physiol.* **130,** 401–409
19. Okada, Y., Maeno, E., Shimizu, T., Dezaki, K., Wang, J., and Morishima, S. (2001) *J. Physiol.* **532,** 3–16
20. Liang, D., Bhatta, S., Gerzanich, V., and Simard, J. M. (2007) *Neurosurg. Focus* **22,** E2
21. Gerzanich, V., Woo, S. K., Vennekens, R., Tsymbalyuk, O., Ivanova, S., Ivanov, A., Geng, Z., Chen, Z., Nilius, B., Flockerzi, V., Freichel, M., and Simard, J. M. (2009) *Nat. Med.* **15,** 185–191
22. Simard, J. M., Chen, M., Tarasov, K. V., Bhatta, S., Ivanova, S., Melnitchenko, L., Tsymbalyuk, N., West, G. A., and Gerzanich, V. (2006) *Nat. Med.* **12,** 433–440
23. Brummelkamp, T. R., Bernards, R., and Agami, R. (2002) *Science* **296,** 550–553
24. Launay, P., Cheng, H., Srivatsan, S., Penner, R., Fleig, A., and Kinet, J. P. (2004) *Science* **306,** 1374–1377
25. Fonfria, E., Murdock, P. R., Cusdin, F. S., Benham, C. D., Kelsell, R. E., and McNulty, S. (2006) *J. Recept. Signal. Transduct. Res.* **26,** 159–178
26. Hetz, C., Bono, M. R., Barros, L. F., and Lagos, R. (2002) *Proc. Natl. Acad. Sci. U.S.A.* **99,** 2696–2701
27. Crowe, W. E., Altamirano, J., Huerto, L., and Alvarez-Leefmans, F. J. (1995) *Neuroscience* **69,** 283–296
28. Stutzin, A., Torres, R., Oporto, M., Pacheco, P., Eguiguren, A. L., Cid, L. P., and Sepúlveda, F. V. (1999) *Am. J. Physiol. Cell Physiol.* **277,** C392–C402
29. Laemmli, U. K. (1970) *Nature* **227,** 680–685
30. Nilius, B., Prenen, J., Tang, J., Wang, C., Owsianik, G., Janssens, A., Voets, T., and Zhu, M. X. (2005) *J. Biol. Chem.* **280,** 6423–6433
31. Varela, D., Simon, F., Riveros, A., Jørgensen, F., and Stutzin, A. (2004) *J. Biol. Chem.* **279,** 13301–13304
32. Guinamard, R., Demion, M., Magaud, C., Potreau, D., and Bois, P. (2006) *Hypertension* **48,** 587–594
33. Prawitt, D., Monteilh-Zoller, M. K., Brixel, L., Spangenberg, C., Zabel, B.,

Fleig, A., and Penner, R. (2003) *Proc. Natl. Acad. Sci. U.S.A.* **100,** 15166–15171

34. Claiborne, A., Yeh, J. I., Mallett, T. C., Luba, J., Crane, E. J., 3rd, Charrier, V., and Parsonage, D. (1999) *Biochemistry* **38,** 15407–15416

35. Poole, L. B., Karplus, P. A., and Claiborne, A. (2004) *Annu. Rev. Pharmacol. Toxicol.* **44,** 325–347

36. Salsbury, F. R., Jr., Knutson, S. T., Poole, L. B., and Fetrow, J. S. (2008) *Protein Sci.* **17,** 299–312

37. Wang, J., Weigand, L., Lu, W., Sylvester, J. T., Semenza, G. L., and Shimoda, L. A. (2006) *Circ. Res.* **98,** 1528–1537

38. Lin, M. J., Leung, G. P., Zhang, W. M., Yang, X. R., Yip, K. P., Tse, C. M., and Sham, J. S. (2004) *Circ. Res.* **95,** 496–505

39. Aarts, M., Iihara, K., Wei, W. L., Xiong, Z. G., Arundine, M., Cerwinski, W., MacDonald, J. F., and Tymianski, M. (2003) *Cell* **115,** 863–877

40. Hara, Y., Wakamori, M., Ishii, M., Maeno, E., Nishida, M., Yoshida, T., Yamada, H., Shimizu, S., Mori, E., Kudoh, J., Shimizu, N., Kurose, H., Okada, Y., Imoto, K., and Mori, Y. (2002) *Mol. Cell* **9,** 163–173

41. Kolisek, M., Beck, A., Fleig, A., and Penner, R. (2005) *Mol. Cell* **18,** 61–69

42. Galluzzi, L., Maiuri, M. C., Vitale, I., Zischka, H., Castedo, M., Zitvogel, L., and Kroemer, G. (2007) *Cell Death Differ.* **14,** 1237–1243